A Method for Efficiently Solving the IAST Equations with an Application to Adsorber Dynamics

Héctor Octavio Rubiera Landa and Dietrich Flockerzi
Max Planck Institute for Dynamics of Complex Technical Systems, Sandtorstr. 1, 39106 Magdeburg, Germany

Andreas Seidel-Morgenstern
Max Planck Institute for Dynamics of Complex Technical Systems, Sandtorstr. 1, 39106 Magdeburg, Germany

Institut für Verfahrenstechnik, Otto-von-Guericke-Universität Magdeburg, Universitätsplatz 2, D-39106 Magdeburg, Germany

DOI 10.1002/aic.13894
Published online September 4, 2012 in Wiley Online Library (wileyonlinelibrary.com).

The Ideal Adsorbed Solution Theory (IAST) developed by Myers and Prausnitz and Radke and Prausnitz provides a powerful tool to calculate multicomponent adsorption equilibria based on single component adsorption isotherms. An important aspect of the application of IAST is that it requires the solution of an implicit algebraic system of equations. Analytical solutions can be derived only for few simple single component isotherm models. This work offers a new concept to solve the equations of the IAST for mixtures of N *components characterized by nondecreasing single component adsorption isotherm behavior. The approach is based on transforming the algebraic system of IAST equations to a system of ODEs with one specified initial value. This work also provides analytical expressions for the partial derivatives of the predicted adsorption equilibria and increases the efficiency of numerical calculations for fixed-bed adsorber dynamics. The strength of the solution method is illustrated in case studies.* © 2012 American Institute of Chemical Engineers *AIChE J,* 59: 1263–1277, 2013

Keywords: separations, thermodynamics, adsorption equilibria, ideal adsorbed solution theory, adsorber dynamics

Introduction

The knowledge about the specific equilibrium functions is an essential prerequisite to properly design adsorption-based separation processes. Adsorption isotherms quantify the distribution of components between the fluid and solid phases at constant temperature.

The experimental determination of adsorption isotherm functions is a time-consuming and difficult task. It is, therefore, of considerable interest to predict these functions applying theoretical tools. Although tremendous progress has been made in the last years in this field, a reliable prediction of adsorption equilibria is still a challenging task, in particular for industrially applied adsorbents characterized by significant degrees of nonuniformity.

To minimize experimental efforts, the following concept is typically applied to describe multicomponent adsorption isotherms. First, the ''easier-to-measure'' single component isotherms are measured, exploiting the wide arsenal of available experimental methods.[1,2] Next, these isotherms are evaluated to identify and parametrize single component adsorption isotherm equations, which describe, as accurately as possible, the acquired experimental information. Subsequently, to avoid the tedious and difficult task of measuring multicomponent adsorption equilibrium data, thermodynamic concepts are applied to predict the corresponding competitive isotherms, typically exploiting simplifying assumptions regarding the state of the phases involved.

The Ideal Adsorbed Solution Theory (IAST), developed in 1965 by Myers and Prausnitz,[3] is the most successful concept in this regard. It was originally developed to describe gas phase adsorption and later extended by Radke and Prausnitz[4] to describe adsorption equilibria for diluted liquid solutions. Besides this theory, other approaches have been suggested; for example, the Vacancy Solution Theory (VST) by Suwanayuen and Danner[5] and the theory of heterogeneous solid surfaces.[6] However, none of these alternatives has achieved the popularity of IAST.

An important drawback related to the application of IAST is due to the fact that it provides an implicit set of equations, which, in general, has no closed solution. The IAST equations can be solved analytically only for a few very simple single component adsorption isotherm models. This aspect has triggered several activities during the last years devoted to overcome mathematical problems in the application of IAST. However, no completely satisfying solution is available yet. This is the motivation for our study: we reformulate the IAST equations in a way that allows an alternative simple and reliable solution concept.

This article is structured as follows. In the section entitled Introduction, we briefly introduce the IAST equations and summarize a few of the available solution concepts. The section entitled Ideal Adsorbed Solution Theory Equations

Correspondence concerning this article should be addressed to A. Seidel-Morgenstern at seidel-morgenstern@mpi-magdeburg.mpg.de.

introduces and demonstrates our approach for the efficient computation of adsorption equilibria using IAST. Lastly, in the section entitled Dynamic Modeling of Fixed-Bed Adsorbers Using IAST we address an application to fixed-bed adsorber dynamics. We derive analytical expressions for the Jacobian of the adsorbed phase concentrations as functions of the fluid phase concentrations when the equilibrium is given by IAST. These expressions simplify the calculation of fixed-bed adsorber dynamics with equilibrium-based models.

Ideal Adsorbed Solution Theory Equations

To present the IAST for ideal fluid phases (gases or liquids), we start with Raoult's law for adsorption. We formulate this law for a system consisting of a liquid phase and an adsorbed phase. For an adsorbable component i at equilibrium we can write

$$c_i = c_i^0(T,\pi)\, x_i, \quad i = 1,\ldots,N \tag{1}$$

Expression 1 states that the equilibrium concentration in the liquid phase, c_i, is directly proportional to a hypothetical liquid phase concentration, c_i^0, of the pure component i at the equilibrium temperature, T, and equilibrium spreading pressure of the system, π, times the molar fraction, x_i, of the component in the adsorbed phase. Likewise, we could perform the analysis for adsorption from an ideal gas phase by substituting the liquid phase concentrations by partial pressures (i.e., $c_i = p_i$, $c_i^0 = p_i^0$).

We require that all molar fractions, x_i, sum up to unity

$$\sum_{i=1}^{N} \frac{c_i}{c_i^0} = \sum_{i=1}^{N} x_i = 1 \tag{2}$$

It is, therefore, necessary in principle to know the spreading pressure, π, of the system to be able to calculate the molar fractions of the components in the adsorbed phase. From the Gibbs adsorption isotherm for a component i we have

$$A\, d\pi = q_i\, d\mu_i^a \tag{3}$$

where q_i denotes the molar concentration of component i in the adsorbed phase. Equilibrium thermodynamics states that the chemical potential of a component, μ_i, should be the same for all phases that constitute the system (the fluid and adsorbed phases), which means for the case of diluted liquid solutions

$$\mu_i^{\mathrm{a}} = \mu_i^{\ell} = \mu_i^{\mathrm{ref}} + RT \ln \frac{c_i}{c_i^{\mathrm{ref}}} \tag{4}$$

The superscripts a and ℓ indicate the adsorbed and the fluid phases, respectively; superscript ref indicates a reference state. We can substitute Eq. 4 in Eq. 3 and integrate to express the spreading pressure for a finite concentration c_i^0

$$\frac{A\pi_i(c_i^0)}{RT} = \int_0^{c_i^0} \frac{q_i^0(s)}{s}\, ds \tag{5}$$

This concentration c_i^0 is a key information of IAST. It represents the hypothetical concentration that component i alone should possess to generate the same spreading pressure as all components do in the mixture. To use Eq. 5 to compute the spreading pressure, adsorbed phase concentrations, q_i^0, are needed for all liquid phase concentrations between 0 and c_i^0, that is, the adsorption isotherms. Instead of π_i, we will use in what follows the modified spreading pressure, Π_i

$$\Pi_i(c_i^0) = \frac{A\pi_i(c_i^0)}{RT} \tag{6}$$

The IAST states that equilibrium is reached when all components i exert at their hypothetical liquid phase concentration, c_i^0, the same modified spreading pressure

$$\Pi := \Pi_1(c_1^0) \stackrel{!}{=} \ldots \stackrel{!}{=} \Pi_N(c_N^0) \tag{7}$$

An ideal adsorbed solution also implies that there should be no changes in the area covered by each component in the adsorbed phase due to mixing with other adsorbates, that is, the area used for adsorption is the same if the component is in a mixture with other adsorbates, as if the component is found in pure form at the temperature and spreading pressure of the mixture. Therefore, the following relation holds

$$\frac{1}{q_{\mathrm{tot}}} = \sum_{i=1}^{N} \frac{x_i}{q_i^0} = \sum_{i=1}^{N} \frac{c_i}{c_i^0 q_i^0(c_i^0)} \tag{8}$$

With the total adsorbed phase concentration, $q_{\mathrm{tot}} = q_{\mathrm{tot}}(c,c^0)$, given by Eq. 8, and with the adsorbate molar fractions, $x_1, \ldots, x_N$, the specific adsorbed phase concentrations, $q_i = q_i(c,c^0)$, are given by

$$q_i = q_{\mathrm{tot}} x_i, \quad i = 1,\ldots,N \tag{9}$$

Equations 1, 2, 7, 8, and 9 provide a complete description of the multicomponent adsorption equilibrium by means of IAST. Substitution of Eq. 8 in Eq. 9 finally yields

$$q_i(c,c^0) = \left[\sum_{k=1}^{N} \frac{c_k}{c_k^0 q_k^0(c_k^0)}\right]^{-1} \cdot \left[\frac{c_i}{c_i^0}\right], \quad i = 1,\ldots,N \tag{10}$$

To express the adsorbed phase equilibrium concentrations, $q = (q_1, \ldots, q_N)^T$, for given liquid phase equilibrium concentrations, $c_1, \ldots, c_N$, one first solves Eqs. 2 and 7 together with Eqs. 5 and 6 for the vector c^0 of the hypothetical liquid phase concentrations as function of $c = (c_1,\ldots c_N)^T$ and then uses Eq. 10 to define the adsorbed phase equilibrium concentrations q as a function of c.

Different alternatives to solve this problem are discussed next. They will reveal issues related to the following Items:

(I1) Integration of Eq. 5.

(I2) Inversion of the resulting $\Pi(c_i^0)$ to obtain c_i^0 as a function of Π, Eq. 7.

(I3) Initialization of the numerical method for solving specific (i.e., method-dependent) nonlinear algebraic equations.

In the following, we will briefly introduce some of the reported solution approaches.

Approach of O'Brien and Myers (FastIAS)[7–9]

O'Brien and Myers study carefully the structure of Eqs. 1, 2, 5, 7, and 8 and introduce two key ideas to efficiently deal with IAST.

- First concept (FastIAS). Express the spreading pressures as a system of $N-1$ equalities

$$\Pi_1(c_1^0) = \Pi_2(c_2^0), \quad \Pi_2(c_2^0) = \Pi_3(c_3^0), \ldots, \quad \Pi_{N-2}(c_{N-2}^0) = \Pi_{N-1}(c_{N-1}^0) \tag{11a}$$

The system of equations to be solved is completed with the relation provided by the closure condition

$$\sum_{i=1}^{N} \frac{c_i}{c_i^0} = 1 \tag{11b}$$

The Eqs. 11 constitute a system of N nonlinear algebraic equations, $G(c^0) = 0$. This system of equations is solved numerically, for example, with the Newton-Raphson method, thus suitable starting values, $c^{0,\text{start}}$, as well as the Jacobian matrix of G with respect to the arguments c^0 are needed.

• Second concept (Modified FastIAS). The system 11 can also be written as

$$\Pi_1(c_1^0) = \Pi_2(c_2^0), \quad \Pi_1(c_1^0) = \Pi_3(c_3^0), \ldots, \quad \Pi_1(c_1^0) = \Pi_N(c_N^0) \tag{12a}$$

$$\sum_{i=1}^{N} \frac{c_i}{c_i^0} = 1 \tag{12b}$$

The modified system 12 has the advantage that its Jacobian matrix now has a simple sparse structure decreasing the number of operations to be performed and, therefore, the computation time.

This approach is effective when modified spreading pressures, $\Pi_i(c_i^0)$, can be integrated analytically. For several single component adsorption isotherm models, however, the modified spreading pressure can only be computed with numerical quadrature (cf., Item (I1) mentioned above). Furthermore, an adequate strategy to provide an initial guess, $c^{0,\text{start}}$, is essential for this method. O'Brien and Myers[7] suggest the following one

$$c_k^{0,\text{start}} = \frac{\sum_{i=1}^{N} B_i c_i}{B_k}, \quad k = 1, \ldots, N \tag{13}$$

with $B_k \equiv \lim_{c_k^0 \to 0} \frac{dq_k^0(c_k^0)}{dc_k^0}$. This initialization strategy may not guarantee convergence in the case of general adsorption isotherm shapes.

Approach of Myers[9,10] and Do[11]

In this approach, we use the closure condition 2 to reduce the problem to a single nonlinear algebraic equation in Π

$$\frac{c_1}{c_1^0(\Pi)} + \cdots + \frac{c_N}{c_N^0(\Pi)} = 1 \tag{14}$$

Therefore, we first perform the integration of 5 to obtain $\Pi(c_i^0)$. For the further discussion of 14, we need the inverse $c_i^0(\Pi)$.

For simple single component adsorption isotherms, the integration and the inversion are straightforward.

For example, for a single component Langmuir isotherm of the form

$$q_i^0 = q_i^{\text{sat}} \frac{b_i c_i^0}{1 + b_i c_i^0}, \quad i = 1, \ldots, N \tag{15}$$

assuming $q^{\text{sat}} = q_1^{\text{sat}} = \ldots = q_N^{\text{sat}}$ and using Eqs. 5 and 6, that is,

$$\Pi(c_i^0) = q^{\text{sat}} \int_0^{c_i^0} \frac{b_i}{1 + b_i s} ds, \quad i = 1, \ldots, N \tag{16}$$

we obtain by integration

$$\Pi(c_i^0) = q^{\text{sat}} \ln\left[1 + b_i c_i^0\right] \tag{17}$$

Now we invert Eq. 17 to obtain

$$c_i^0(\Pi) = \frac{\exp\left[\frac{\Pi}{q^{\text{sat}}}\right] - 1}{b_i} \tag{18}$$

These expressions are introduced into Eq. 14 and, thus, lead to the classic multicomponent Langmuir adsorption isotherm

$$q_i(c_1, c_2) = q^{\text{sat}} \frac{b_i c_i}{1 + b_1\, c_1 + b_2\, c_2}, \quad i = 1, 2 \tag{19}$$

Equation 19 was originally derived from adsorption kinetics arguments.[1] For the single component Langmuir model, IAST provides the same result.

Analogously, for the single component quadratic adsorption isotherm model

$$q_i^0(c_i^0) \equiv q_i^0 = q^{\text{sat}} \frac{c_i^0\left(b_{i1} + 2\, b_{i2}\, c_i^0\right)}{1 + b_{i1}\, c_i^0 + b_{i2}\, c_i^{0\,2}}, \quad i = 1, \ldots, N \tag{20}$$

with modified spreading pressure

$$\Pi(c_i^0) = q^{\text{sat}}\ \ln\left[1 + b_{i1}\, c_i^0 + b_{i2}\, c_i^{0\,2}\right] \tag{21}$$

we have

$$c_i^0(\Pi) = -\frac{1}{2}\frac{b_{i1}}{b_{i2}} + \sqrt{\frac{1}{4}\left(\frac{b_{i1}}{b_{i2}}\right)^2 + \frac{1}{b_{i2}}\left(\exp\left[\frac{\Pi}{q^{\text{sat}}}\right] - 1\right)}, \quad i = 1, \ldots, N \tag{22}$$

and we insert this result in 14 as before.

In the case of more complex adsorption isotherm models, it may not be possible to solve explicitly for $c_i^0(\Pi)$ (cf., Item (I2)) and one has to apply numerical inversion.

To initialize the iterations for Eq. 14 (cf., Item (I3)), it is suggested that the modified spreading pressure be evaluated at the total fluid phase concentration, c_{tot}

$$\Pi^{\text{start}} = \sum_{i=1}^{N} \frac{c_i}{c_{\text{tot}}} \cdot \int_0^{c_{\text{tot}}} \frac{q_i^0(s)}{s} ds, \quad i = 1, \ldots, N \tag{23}$$

Analytical approach of Ilić et al.[12]

Recently, Ilić et al. derived an explicit solution of the IAST equations for the calculation of adsorbed phase concentrations of binary systems whose individual component behavior is represented by second-order (quadratic) adsorption isotherms given by Eq. 20. This type of flexible single component equilibrium model allows the description of inflection points in the course of an isotherm. We present this solution here to set the stage for the alternative concept introduced in the next section. The equality $\Pi(c_1^0) = \Pi(c_2^0)$ yields for the quadratic model 20

$$\int_0^{c_1^0} \frac{b_{11} + 2\, b_{12}\, s}{1 + b_{11}\, s + b_{12}\, s^2}\, ds = \int_0^{c_2^0} \frac{b_{21} + 2\, b_{22}\, s}{1 + b_{21}\, s + b_{22}\, s^2}\, ds \quad (24)$$

These expressions are integrated analytically. Using the closure condition we obtain

$$1 + b_{11}\, c_1^0 + b_{12}\, c_1^{0\,2} = 1 + b_{21}\left[\frac{c_2\, c_1^0}{c_1^0 - c_1}\right] + b_{22}\left[\frac{c_2\, c_1^0}{c_1^0 - c_1}\right]^2 \quad (25)$$

We write Eq. 25 in standard polynomial form

$$\mathcal{P}\left(\frac{c_1}{c_1^0}\right) = a_1(c_1,\, c_2)\left[\frac{c_1}{c_1^0}\right]^3 + a_2(c_1,\, c_2)\left[\frac{c_1}{c_1^0}\right]^2 + a_3(c_1, c_2)\left[\frac{c_1}{c_1^0}\right] + a_4(c_1,\, c_2) = 0 \quad (26)$$

with coefficients defined by $a_1(c_1,c_2) = \alpha\, c_1 + c_2$, $a_2(c_1,c_2) = c_1\,[\beta\, c_1 - 2\alpha] - c_2\,[1 + \gamma\, c_2]$, $a_3(c_1,c_2) = c_1\,[\alpha - 2\,\beta\, c_1]$, $a_4(c_1,c_2) = \beta\, c_1^2$, and the constants $\alpha = \frac{b_{11}}{b_{21}} > 0$, $\beta = \frac{b_{12}}{b_{21}} \geq 0$ and $\gamma = \frac{b_{22}}{b_{21}} \geq 0$. The roots of this polynomial can be derived analytically by applying the formulae of Cardano. The problem is solved by selecting the physically meaningful root.[12] We observe that with this type of ansatz, we have introduced the original liquid phase concentrations (c_1, c_2) in the form of parameters to the problem.

Along the same line of thought, Tarafder and Mazzotti[13] have recently presented a method to obtain explicit (i.e., analytical) isotherms for binary systems using IAST when the single component adsorption isotherms are of the following types: Langmuir, anti-Langmuir, Brunauer-Emmett-Teller, and quadratic.

The New Approach

We will now introduce a new concept to solve the equations of the IAST for mixtures of N components characterized by general, continuously differentiable, single component adsorption isotherms with the following property

$$\Pi_i(c_i^0) \to \infty \quad \text{for } c_i^0 \to \infty, \quad i = 1, \ldots, N \quad (27a)$$

The single component adsorption isotherms, $q_i^0(c_i^0)$, are positive except for $q_i^0(0) = 0$ with

$$\frac{dq_i^0}{dc_i^0}(0) > 0 \quad (27b)$$

We also start with Eq. 7, which states that the spreading pressure exerted by every adsorbate at the hypothetical liquid phase concentrations, c_i^0, should be the same. As in the approach of Ilić et al.[12] our goal is to express the hypothetical liquid phase concentrations as functions of one of them, for example,

$$c_k^0 = c_k^0(c_1^0), \quad k = 2, 3, \ldots, N \quad (28)$$

This is possible in closed form when we can compute and invert $\pi_k(c_k^0)$ explicitly. In Ilić et al.[12] this results in a third-order polynomial with analytical formulas for the zeros. For the suggested new approach, we first formulate Eq. 7 as in the Modified FastIAS approach[8]

$$\Pi_1(c_1^0) = \Pi_2(c_2^0) \quad (29a)$$

$$\Pi_1(c_1^0) = \Pi_3(c_3^0) \quad (29b)$$

$$\vdots \quad (29c)$$

$$\Pi_1(c_1^0) = \Pi_N(c_N^0) \quad (29d)$$

This results in $N - 1$ equalities. Now, let us suppose that we have a solution $c_k^0 = c_k^0(c_1^0)$ with $c_k^0(0) = 0$ satisfying

$$\Pi_k(c_k^0(c_1^0)) = \Pi_1(c_1^0), \quad \Pi_k(c_k^0(0)) = \Pi_1(0) = 0, \quad k = 2, 3, \ldots, N \quad (30)$$

We proceed in a dynamic way by differentiating these expressions

$$\Pi_k'(c_k^0(c_1^0))\frac{dc_k^0(c_1^0)}{dc_1^0} = \Pi_1'(c_1^0), \quad k = 2, \ldots, N \quad (31)$$

Hence, we arrive at $N - 1$ decoupled non-autonomous initial value problems

$$\frac{dc_k^0}{dc_1^0} = \frac{\Pi_1'(c_1^0)}{\Pi_k'(c_k^0)} = \frac{q_1^0(c_1^0)/c_1^0}{q_k^0(c_k^0)/c_k^0}, \quad c_k^0(0) = 0, \quad k = 2, 3, \ldots, N \quad (32a)$$

which are supplemented by the trivial initial value problem

$$\frac{dc_k^0}{dc_1^0} = 1, \quad c_k^0(0) = 0 \quad \text{for } k = 1 \quad (32b)$$

possessing the solution c_1^0.

What we have accomplished is the transformation of our original set of algebraic equations into the non-autonomous initial value problem 32. The N-dimensional solution $c^0 = \psi(c_1^0)$ of the initial value problem 32 is the sought solution of 29 (by separation of variables). So we arrive at a representation of the form 28 circumventing the issues addressed in the section entitled Ideal Adsorbed Solution Theory Equations (Items (I1) - (I3)).

We now turn to the expression that relates both the hypothetical equilibrium concentrations, $c^0 = (c_1^0,\ldots,c_N^0)^T$, and the given liquid phase concentrations, $c = (c_1,\ldots,c_N)^T$. It is given by the closure condition, Eq. 2, which we restate here again for completeness

$$\sum_{k=1}^{N} x_k = \frac{c_1}{c_1^0} + \cdots + \frac{c_N}{c_N^0} = 1 \quad (33)$$

This closure condition is such that, given a particular set of liquid phase concentrations $(c_1, \ldots\ c_N)^T$, the solution $c^0 = \psi(c_1^0)$ cuts the surface 33 in the positive octant just once and transversely by 28. This is illustrated in Figure 1 for the case of a ternary mixture. The intersection point $c_1^0 = c_1^0(c_1,\ldots,c_N)$ satisfies the scalar equation

$$\frac{c_1}{\psi_1(c_1^0)} + \cdots + \frac{c_N}{\psi_N(c_1^0)} = 1 \quad (34)$$

and provides the hypothetical equilibrium liquid phase concentrations

$$c_k^0 = \psi_k(c_1^0(c_1, \ldots, c_N)), \quad k = 1, \ldots, N \quad (35)$$

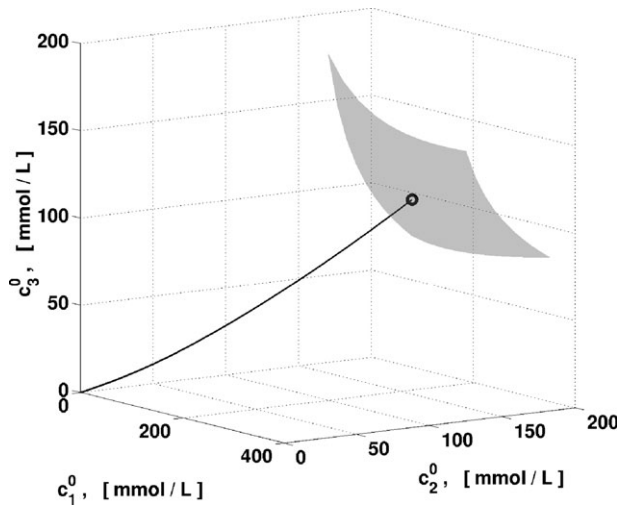

Figure 1. Illustration of the new approach for a mixture consisting of three phenyl-*n*-alcanes with the isotherm model given by Eq. 60 and discussed in section entitled Dynamic Modeling of Fixed-Bed Adsorbers Using IAST.

Compound 1: phenyl-*n*-octane (c_1^0), compound 2: phenyl-*n*-decane (c_2^0), and compound 3: phenyl-*n*-undecane (c_3^0). The corresponding single component adsorption isotherms of these compounds are shown in Figure 4 with parameters given in Table 7. Solid line: solution segment of (32) corresponding to Eq. A3. Gray surface: closure condition. The circle indicates the solution c^0 = {236.0 mmol/l, 145.0 mmol/l, 112.8 mmol/l} for given c = {50.0 mmol/l, 50.0 mmol/l, 50.0 mmol/l}. With these values, we obtain the adsorbed phase equilibrium concentrations $q(c)$ = {61.5 mmol/l, 100.1 mmol/l, 129.0 mmol/l}.

as a function of $c = (c_1,\ldots,c_N)^T$. With c^0 from (35), we can now express the adsorbed phase equilibrium concentration, $q = (q_1, \ldots, q_N)^T$, as function of c using Eq. 10. If the liquid phase concentrations change from $(c_1,\ldots,c_N)^T$ to $\hat{c} = (\hat{c_1}, \ldots \hat{c_N})^T$, a new adsorption equilibrium state is established, requiring new hypothetical equilibrium liquid phase concentrations on the solution $c^0 = \psi(c_1^0)$ of the (unchanged) initial value problem 32. Any point along this solution can be taken as a valid starting point for a numerical routine to solve the closure condition (34). In case of $\sum \frac{\hat{c}_k}{c_k^0(c)} > 1$, one moves from $\psi(c_1^0)$ along the solution of 32 in the positive c_1^0-direction until Eq. 34 is met for the first ''time'', say at $c_1^0 = c_1^0(\hat{c})$. One then defines $c^0 = \psi(c_1^0(\hat{c}))$ as in (35) and finally $q(c)$ as in 10 in dependence of $\hat{c}$. In case of $\sum \frac{c_k}{c_k^0(c)} < 1$, one proceeds in complete analogy by moving in the negative c_1^0-direction along the solution of 32. For a more compact notation and for an ''integration'' of the closure condition (33) into the initial value problem 32 we refer to Appendix A, in particular to Eq. A3.

Before illustrating some examples, we would like to state also that our approach works when the task consists of calculating the fluid phase concentrations, c, given the adsorbed phase concentrations, q. Assuming that the $q_i^0(c_i^0)$ are inverted to give $c_i^0(q_i^0)$, Eq. 7 can be written as[14]

$$\Pi := \tilde{\Pi}_1(q_1^0) \stackrel{!}{=} \ldots \stackrel{!}{=} \tilde{\Pi}_N(q_N^0),$$

$$\tilde{\Pi}(q_i^0) = \int_0^{q_i^0} \frac{s}{c_i^0(s)} \frac{dc_i^0(s)}{ds}\, ds = \int_0^{q_i^0} \frac{d \ln c_i^0(s)}{d \ln s}\, ds \tag{36}$$

The corresponding closure condition is given by (2)

$$\frac{q_1}{q_1^0} + \cdots + \frac{q_N}{q_N^0} = 1 \tag{37}$$

The solution $q^0 = \tilde{\psi}(q)$ of Eqs. 36 and 37 can be obtained by our approach via the analoga to Eqs. 32 and A3. The sought liquid phase concentrations, $c = c(q)$, are given by 9 and hence by

$$c_i = c_i^0(q^0) \cdot \frac{q_i}{q_{\text{tot}}}, \quad i = 1, \ldots, N \tag{38}$$

Example 1: Illustration

We want to assess the efficiency of the new proposed approach and illustrate the concepts introduced above. We consider a binary system where the single component adsorption behavior is described by the Langmuir isotherm model. Let us start with Eq. 7, that is, $\Pi_1(c_1^0) = \Pi_2(c_2^0)$. Substituting the single component Langmuir isotherm, Eq. 15, and letting $q^{\text{sat}} = q_1^{\text{sat}} = q_2^{\text{sat}}$, yields

$$\int_0^{c_1^0} \frac{b_1}{1 + b_1\, s}\, ds = \int_0^{c_2^0} \frac{b_2}{1 + b_2\, s}\, ds \tag{39}$$

Integrating both sides holds

$$c_1^0(c_2^0) = \frac{b_2}{b_1}\, c_2^0 \tag{40}$$

This expression can then be substituted into the closure condition 2 to find a particular hypothetical liquid phase concentration, c_i^0, for specified liquid phase concentrations, c_1, c_2

$$c_1^0 = c_1 + \frac{b_2}{b_1}\, c_2 \tag{41}$$

The adsorbed phase concentration values q_1, q_2 are computed from the remaining Eq. 10. A simple algebraic manipulation leads us to Eq. 19.

We now follow the new proposed strategy as outlined at the beginning of this Section, starting again from Eq. 7

$$\Pi_2\big(c_2^0(c_1^0)\big) = \Pi_1\big(c_1^0\big) \tag{42}$$

Differentiation gives

$$\Pi_2'\, \frac{dc_2^0}{dc_1^0} = \Pi_1' \tag{43}$$

and, thus,

$$\frac{dc_2^0}{dc_1^0} = \frac{\Pi_1'}{\Pi_2'} = \frac{q_1^0/c_1^0}{q_2^0/c_2^0} = \frac{\frac{b_1}{1+b_1c_1^0}}{\frac{b_2}{1+b_2c_2^0}} \tag{44}$$

We set-up the following initial value problem, (cf., Eq. 32)

$$\frac{dc_1^0}{dc_1^0} = 1 \tag{45a}$$

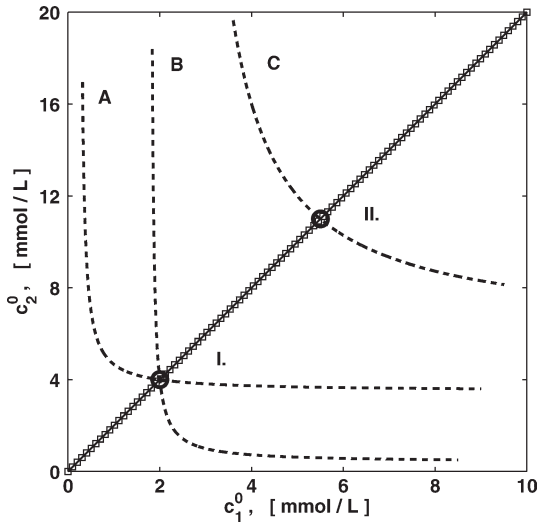

Figure 2. Illustration of the new approach for a mixture.

A Langmuir single component isotherm model, Eq. 15, was taken for both species with the following parameters: $q^{sat} = q_1^{sat} = q_2^{sat} = 1$ mmol/l, $b_1 = 2$ l/mmol and $b_2 = 1$ l/mmol. Continuous line/Squares: analytical/numerical solution of 45. Dotted lines A, B, and C are the hypersurfaces (i.e., hyperbolas) given by the closure condition (33) with transverse intersections at points I. (A & B) and II. (C). Hyperbola A: $\{c_1, c_2\} = \{0.25,3.5\}$. Hyperbola B: $\{c_1, c_2\} = \{1.8,0.4\}$. Hyperbola C: $\{c_1, c_2\} = \{2.5,6.0\}$. Point I: $\{c_1^0, c_2^0\} = \{2.0,4.0\}$. Point II: $\{c_1^0, c_2^0\} = \{5.5,11.0\}$. Concentration values are in mmol/l.

$$\frac{dc_2^0}{dc_1^0} = \frac{b_1\left(1 + b_2\, c_2^0\right)}{b_2\left(1 + b_1\, c_1^0\right)} \tag{45b}$$

$$c_i^0(0) = 0, \quad i = 1,2 \tag{45c}$$

The solution of the initial value problem 45 is obtained analytically by separation of variables. So we end up with the same expressions as given by 39 and 40. Figure 2 displays the analytical solution 40 of system 45 computed by the new approach.

In this simple example, we can explicitly solve 39 to compute $c_2^0(c_1^0)$. Afterwards, we use Eq. 10 to obtain q_1 and q_2.

Example 2: Accuracy

To explore the accuracy of our new approach we turn to the analytical solution of Ilić et al.[12], introduced above. This is our reference solution and is used to compare with the new approach and the numerical approaches of O'Brien and Myers[7,8] (FastIAS) and Myers and Do.[10,11] The adsorption isotherm model is given by 20, with the parameters listed in Table 1.

We have used MATLAB (version 7.11.0.584 (R2010b)) to perform our calculations. We executed our programs on a workstation running under Linux, with an Intel Core Quad CPU (Q9550) at 2.83 GHz with 4 GB RAM. Calculations were performed in double-precision arithmetic with floating-point relative accuracy of 2.2204×10^{-16}.

Table 1. Parameters for Example 2 Corresponding to the Quadratic Adsorption Isotherm (Eq. 20), as reported by Ilić et al.[12]

	q^{sat} (g/l)	b_{i1} (l/g)	b_{i2} (l^2/g^2)
Compound 1	5.0	1.0	2.0
Compound 2	5.0	2.0	3.0

Table 2. Maximum Values of the Absolute Computational Error, e_c^{abs} (Eq. 46a), at Specified Error Tolerance(s) for Each Numerical Approach, Calculated for $\hat{q}_1$ (10,000 Equilibrium Points), with Respect to the Reference Solution, q_1

	O'Brien and Myers	Myers and Do	New Approach
Error	9.5×10^{-9}	9.5×10^{-9}	9.5×10^{-9}
Specified tolerance(s)	10^{-4}	10^{-8}	RelTol: 10^{-10}, AbsTol: 10^{-12}

Values in g/l. RelTol and AbsTol refer to the relative and absolute tolerances used with the MATLAB ODE solver, respectively.

We calculated the absolute and relative computational errors

$$e_c^{abs} := |q - \hat{q}| \tag{46a}$$

$$e_c^{rel} := \frac{|q - \hat{q}|}{|q|} \tag{46b}$$

whereby $\hat{q}$ denotes the numerical approximations to the reference (i.e., analytical) adsorbed phase concentrations, q. We computed adsorbed phase equilibria for the liquid phase concentration values $c_i \in [10^{-6}, 10^{1}]$, $i = 1,2$ (concentrations are in g/l). These intervals were partitioned equidistantly to generate discrete input values (with sub-indices $m,n = 1,2, \ldots, 100$), $\{c_{1,(m)}, c_{2,(n)}\}$, to compute 100×100 adsorbed phase concentrations of the analytical solution q_1 $\{c_{1,(m)},c_{2,(n)}\}$, q_2 $\{c_{1,(m)},c_{2,(n)}\}$, as well as the numerical solutions $\hat{q}_1$ $\{c_{1,(m)},c_{2,(n)}\}$, $\hat{q}_2$ $\{c_{1,(m)},c_{2,(n)}\}$ (analogously to the adsorbed phase concentration surfaces shown in Figures 5b,c).

The maximum computed absolute and relative errors for the numerical solutions $\hat{q}_1$ are given in Tables 2 and 3. Values of these errors were also calculated for $\hat{q}_2$, which were similar in order of magnitude and, therefore, not included for brevity.

In the O'Brien and Myers approach, we need to specify a single error tolerance for the iteration of the Newton-Raphson method. In the case of the Myers and Do approach, the reported error tolerance in Tables 2 and 3 was used in two iterations: numerical inversion (i.e., compute $c_i^0(\Pi)$) and the (external) iteration that computes the modified spreading pressure, Π from the closure condition (cf., Eq. 14). In the case of the new approach, we computed with the ODE

Table 3. Maximum Values of the Relative Computational error, e_c^{rel} (Eq. 46b), at Specified Error Tolerance(s) for Each Numerical Approach, Calculated for $\hat{q}_1$ (10,000 Equilibrium Points), with Respect to the Reference Solution, q_1

	O'Brien and Myers	Myers and Do	New Approach
Error	8.7×10^{-9}	3.3×10^{-7}	9.8×10^{-10}
Specified tolerance(s)	10^{-4}	10^{-8}	RelTol: 10^{-10}, AbsTol: 10^{-12}

RelTol and AbsTol refer to the relative and absolute tolerances used with the MATLAB ODE solver, respectively.

Table 4. Parameters Considered by Moon and Tien[15] for the O'Brien and Myers Adsorption Isotherm Model 47

Component, i	q_i^{sat} (mol/kg)	b_i (kPa^{-1})	σ_i (−)
1	5.0	0.01	1.2
2	3.0	0.006	1.1
3	4.0	0.0009	0.8
4	2.0	0.01	1.2
5	3.5	0.003	1.0
6	4.0	0.001	1.1
7	2.0	0.015	1.2
8	2.5	0.001	1.15
9	4.0	0.0001	1.0
10	5.5	0.006	1.0

solver ode45, which allows the user to specify relative and absolute tolerances, designated as RelTol and AbsTol, respectively. We discuss further in Appendix C the effect of these parameters and choice of ODE solver on the calculated solutions using the new approach. We conclude that both standard numerical approaches and the new approach converge well to the analytical solution under appropriate specification of required error tolerances.

Example 3: Calculation Times

We turn now to some of the gas phase adsorption examples given by Moon and Tien[15] and later considered by O'Brien and Myers,[8] which are interesting due to the number of adsorbates in the mixture (3, 5 and 10). For these multicomponent examples there is currently no known analytical solution. The O'Brien and Myers single component adsorption isotherm model [7] (below, c_i^0 is substituted by p_i^0)

$$q_i^0(p_i^0) = q_i^{sat}\left[\frac{b_i p_i^0}{1+b_i p_i^0} + \frac{\sigma_i^2 b_i p_i^0\left(1-b_i p_i^0\right)}{2\left(1+b_i p_i^0\right)^3}\right], \quad i = 1, \ldots, N \tag{47}$$

with modified spreading pressure

$$\Pi(p_i^0) = q_i^{sat}\left[\ln\left[1+b_i\, p_i^0\right] + \frac{\sigma_i^2\, b_i\, p_i^0}{2\left(1+b_i\, p_i^0\right)^2}\right] \tag{48}$$

was used for all components. In particular, we focus on the more challenging 10 component problem with the parameters of Table 4. This task (given in Table V of O'Brien and Myers[8]) consists of calculating adsorbed phase concentrations, q, given the gas phase partial pressures (in kPa): $p_1 = 30.0$, $p_2 = 3.0$, $p_3 = 3.0$, $p_4 = 15.0$, $p_5 = 60.0$, $p_6 = 60.0$, $p_7 = 30.0$, $p_8 = 60.0$, $p_9 = 6.0$, and $p_{10} = 33.0$.

Solving this equilibrium task with the new approach provides complete p^0 information in the pressure range of interest, as shown in Figure 3.

With the inclusion of the closure condition, we easily find the required p^0 values in this 10-dimensional solution space. We then calculate the adsorbed phase equilibrium concentrations, q, with (10). The calculation results are (in mol/kg): $q_1 = 0.8443$, $q_2 = 0.0192$, $q_3 = 0.0043$, $q_4 = 0.0677$, $q_5 = 0.2467$, $q_6 = 0.1093$, $q_7 = 0.2032$, $q_8 = 0.0446$, $q_9 = 0.0010$, and $q_{10} = 0.5739$. We also performed the calculations with the O'Brien and Myers approach (ModifiedFastIAS) and the standard approach of Myers and Do for comparison, obtaining the same results. Table 5 provides the computation times required for each approach.

The new approach has a comparable calculation time to the approach of Myers and Do, which in this case requires numerical inversion (i.e., iteratively) of (48), resulting in additional time cost. The approach of O'Brien and Myers (Modified FastIAS) shows the best result, being roughly 20 times faster than the other two approaches. To be fair to the slower approaches, however, we should keep in mind that Modified FastIAS works specifically for single component adsorption isotherms whose modified spreading pressure is explicit in c_i^0 (cf., Eq. 48).

Example 4: Applicability and Implementation.

There are some inherent difficulties associated with the application of the standard approaches of Myers and Do and O'Brien and Myers:

- inapplicability to a broader class of adsorption isotherm models (cf., Items (I1) and (I2));
- dependency on suitable starting strategies, due to their iterative nature (cf., Item (I3)).

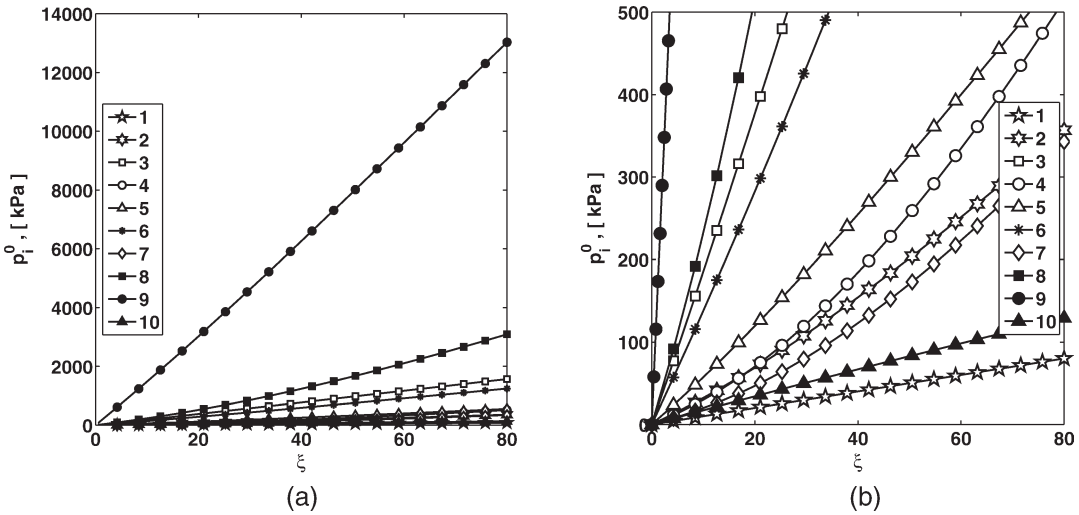

Figure 3. Trajectories for the 10 component case of Example 3.

(a): Solution orbit. and (b): inset of (a) for the low-pressure region.

Table 5. Computation times (seconds) of Each Approach for the Equilibrium State (10 Compounds) Considered in Example 3

Myers and Do	O'Brien and Myers	New Approach
0.38	0.02	0.37

These shortcomings become evident if we consider for instance the Redlich-Peterson single component adsorption isotherm model[16] for a mixture of two adsorbates

$$q_i^0(c_i^0) = \frac{a_i\, c_i^0}{1 + b_i\, c_i^{0\,v_i}}, \quad i = 1, 2 \tag{49}$$

with Henry constant a_i and parameters b_i and v_i. The modified spreading pressure can be expressed in closed form as[17]

$$\Pi(c_i^0) = \frac{a_i/v_i}{b_i^{1/v_i}}\left[\frac{\pi}{\sin(\pi/v_i)} + \sum_{m=1}^{\infty}(-1)^m \frac{\zeta_i^{\,m-(1/v_i)}}{m-(1/v_i)}\right] \tag{50}$$

where $1/v_i \notin \mathbb{N}$, $\pi = 3.14\ldots$, $\zeta_i := \frac{1}{b_i\, c^{0\,v_i}} < 1$. We can automatically discard the O'Brien and Myers approach due to the form of the modified spreading pressure given by (50). With the Myers and Do approach we are confronted again with the difficulty of inverting $\Pi(c_i^0)$, where we would need to truncate the series in Eq. 50 to a sufficient number of terms and then proceed with numerical inversion (i.e., iteratively) to obtain $c_i^0(\Pi)$. The practical implementation based on numerical quadratures increases the calculation times. Additionally, we would require a suitable starting strategy to initialize the iterations (cf., Eq. 23). In contrast, with the new approach, we simply address the initial value problem

$$\frac{dc_1^0}{dc_1^0} = 1, \tag{51a}$$

$$\frac{dc_2^0}{dc_1^0} = \frac{a_1}{a_2}\frac{\left[1 + b_2 c_2^{0\,v_2}\right]}{\left[1 + b_1 c_1^{0\,v_1}\right]} \tag{51b}$$

$$c_i^0(0) = 0, \quad i = 1, 2 \tag{51c}$$

integrate to the desired accuracy to obtain c^0 and compute the adsorbed phase equilibrium concentrations, q, using (10).

An additional difficulty arises when the single component adsorption isotherm models are of different type for each of the adsorbates. This scenario again makes the application of the two standard approaches a cumbersome (if not impossible) task. A sound choice of starting guesses for conventional iterative methods is not clear anymore. This is an important strength of the new approach. We start our calculation (i.e., integration) from a physically valid point of the solution: at zero concentration of all adsorbates.

The examples so far presented allow us to state that the new approach

- results in an easy, straightforward implementation of IAST for general single component adsorption isotherm models;
- does not run into convergence issues (i.e., it is robust)
- ranks well, concerning calculation times, with established calculation procedures.

In the following section, we will address the application of IAST equilibrium calculations to dynamic adsorber modeling. We will further discuss the advantages of the new approach with respect to the standard approaches considered in Examples 2, 3, and 4.

Dynamic Modeling of Fixed-Bed Adsorbers Using IAST

There are various models available that are capable to describe fixed-bed adsorber dynamics. Frequently, several mass-transfer resistances have to be taken into account.[18] To illustrate a specifically attractive feature of our method, we will discuss a simple *equilibrium-based* model under isothermal condition (temperature, T, is constant). In this case, we will require information regarding the first partial derivatives of the adsorbed phase equilibrium concentrations, $q = (q_1, \ldots, q_N)^T$, with respect to the liquid phase concentrations, $c = (c_1, \ldots, c_N)^T$. Let us take a closer look at one of the most frequently applied models of this type, namely, the simple one-parameter, one-dimensional equilibrium dispersive model[19]

$$\frac{\partial c}{\partial t} + \phi\frac{\partial q(c)}{\partial t} + u\frac{\partial c}{\partial z} = D_{\text{app}}\frac{\partial^2 c}{\partial z^2} \tag{52a}$$

with boundary conditions

$$u\, c(t, z=0) - D_{\text{app}}\frac{\partial c}{\partial z}\bigg|_{z=0} = u\, c_{\text{in}}(t), \quad \frac{\partial c}{\partial z}\bigg|_{z=L} = 0 \tag{52b}$$

and initial condition

$$c(t=0, z) = c_0 \tag{52c}$$

for liquid phase concentrations $c = (c_1, \ldots, c_N)^T$, inlet (i.e., injected) concentrations $c_{\text{in}} = (c_{1,\text{in}}, \ldots, c_{N,\text{in}})^T$, adsorbed phase concentrations $q = (q_1, \ldots, q_N)^T$ and apparent dispersion coefficients $D_{\text{app}} = \text{diag}\,(D_{\text{app},1}, \ldots, D_{\text{app},N})$. The mobile phase velocity is defined as $u := \frac{Q}{\epsilon A_c}$, where Q is the volumetric flow rate, ϵ is the total bed porosity, and A_c is the cross-sectional area of the column. We let $\phi = \frac{1-\epsilon}{\epsilon}$ be the phase ratio, that is, the ratio of the column volume occupied by the solid phase with respect to the column volume occupied by the liquid phase. We assume an incompressible mobile liquid phase, isothermal conditions, and instantaneous intraparticle transport. All the effects causing band profile dispersion are lumped onto the apparent dispersion coefficients, $D_{\text{app},k}$.

We recall that for competitive adsorption behavior $q_i = q_i(c_1, \ldots, c_N)$, $i = 1, \ldots, N$. So we apply the chain rule to the time derivative of the adsorbed phase concentration, $\frac{\partial q_i(c)}{\partial t}$, in accordance with the assumption of instantaneous equilibrium, that is

$$\frac{\partial q_i(c)}{\partial t} = \sum_{k=1}^{N}\frac{\partial q_i}{\partial c_k}\frac{\partial c_k}{\partial t}, \quad i = 1, \ldots, N \tag{53}$$

So we can re write the model Eq. 52a as

$$\left[\mathcal{I} + \phi\,\mathcal{J}(q)\right]\frac{\partial c}{\partial t} + u\frac{\partial c}{\partial z} = D_{\text{app}}\frac{\partial^2 c}{\partial z^2} \tag{54}$$

where we have introduced the identity matrix $\mathcal{I}$ of size $N \times N$ and the following Jacobian of the adsorbed phase equilibrium concentrations

$$\mathcal{J}(q) = \begin{pmatrix} \frac{\partial q_1}{\partial c_1} & \cdots & \frac{\partial q_1}{\partial c_N} \\ \vdots & \ddots & \vdots \\ \frac{\partial q_N}{\partial c_1} & \cdots & \frac{\partial q_N}{\partial c_N} \end{pmatrix} \tag{55}$$

Thus, the equilibrium dispersive model given by Eq. 52a can be written as

Table 6. Definitions of the Objects Required for the Computation of the Matrix $\mathcal{K}$, Eq. 59

Object	Expression
Row vector of ones	$e^T = (1,\ldots,1)$
Scaled reciprocal adsorbate concentrations	$w_k := \frac{q_{\text{tot}}}{q_k^0}$, $w = \text{col}\ (w_k)$, $W = \text{diag}\ (w_k)$
Column vector of mole fractions	$x_k := \frac{c_k}{c_k^0}$, $x = \text{col}\ (x_k)$, $X = \text{diag}\ (x_k)$
Scalar σ	$\sigma := \sum_{k=1}^{N} w_k\, c_k\, q_{\text{tot}}\, \frac{d}{dc_k^0}\left(\frac{1}{q_k^0}\right)$
Row vector f^T	$f^T := [w^T\, Wx - \sigma]\, e^T - w^T$
Diagonal matrix $D = D(\lambda)$	$d_k := \frac{q_{\text{tot}}}{\lambda c_k^0 + q_{\text{tot}}}$, $D = \text{diag}\ (d_k)$
Matrix $H = H(\lambda)$	$H := Dx\, f^T - DWx\, e^T$
Scalar $h_1 = h_1(\lambda)$	$h_1 := 1 + \text{tr}\ (H)$
Scalar $h_2 = h_2(\lambda)$	$h_2 := \det\ (I + H)$
Matrix $K_2 = K_2(\lambda)$	$K_2 := \frac{1}{h_2}[h_1\, H\text{-}H^2]$

$$\frac{\partial c}{\partial t} = \left[\mathcal{I} + \phi\ \mathcal{J}(q)\right]^{-1}\left[-u\frac{\partial c}{\partial z} + D_{\text{app}}\frac{\partial^2 c}{\partial z^2}\right] \tag{56}$$

The Proposition of Appendix B shows that, for general nondecreasing isotherms, the Jacobian $\mathcal{J}(q)$ is a hyperbolic matrix possessing N positive eigenvalues with N linearly independent eigenvectors.

When the adsorption equilibrium relationship $q(c)$ has a simple explicit algebraic representation, computing the Jacobian (55) is a straightforward task. When it is not possible to compute this Jacobian analytically, one can resort to a suitable numerical approximation, for example, by an automatic differentiation technique. Another possibility reported by Santos et al.[20] is based on exploiting B-splines to approximate the multicomponent adsorption equilibrium functions, $q(c)$, once they have been computed initially with IAST. In contrast to our approach, described in what follows, the approximated Jacobian is obtained numerically using the computed B-spline coefficients.

It is advantageous to have an analytic preprocessing of the Jacobian of the adsorption equilibrium functions and, in particular, of $[\mathcal{I} + \phi\ \mathcal{J}(q)]^{-1}$. Now, this inverse can be computed analytically from the given single component adsorbed phase concentrations, $q_i^0(c_i^0)$, and their derivatives with respect to c_i^0. Just the evaluation points c are — in general — obtained by a numerical solution of 2 and 7 for example, by a numerical integration of the initial value problem 32 together with the closure condition 33 (cf., Eq. A3 of Appendix A).

The Jacobian $\mathcal{J}(q)$ allows a simple factorization: With the expressions

$$w = [w_1, \ldots, w_N]^T \ \text{ for } \ w_k \equiv w_k(c, c^0) := \frac{q_{\text{tot}}(c, c^0)}{q_k^0(c^0)} \ \text{ and } \quad W := \text{diag}(w_k) \tag{57a}$$

satisfying $w^T x = e^T W x = 1$ (cf., Eq. 8) and the scalar-valued

$$\sigma := \sum_{k=1}^{N} w_k\, c_k q_{\text{tot}}\, \frac{d}{dc_k^0}\left(\frac{1}{q_k^0}\right) \tag{57b}$$

one has

$$\mathcal{J}(q) = \left(\mathcal{I} + J_2\right)\ \text{diag}\left(\frac{q_{\text{tot}}}{c_i^0}\right) \tag{58a}$$

with the matrix

$$\mathcal{I} + J_2 := \left(\mathcal{I} - \left[x\, w^T\right]\right)\left(\mathcal{I} - \left[Wxe^T\right]\right) - \sigma\left[x\, e^T\right] \tag{58b}$$

where J_2 has rank ≤ 2 and where all the terms on the right-hand side of 58 are to be evaluated at c. Here, the dyadic products xw^T, xe^T and Wxe^T define simple rank-1 projections onto the straight lines spanned by x and Wx, respectively. Note that the components $w_k\, x_k$ of the vector Wx are nothing else but $\frac{q_k}{q_k^0}$ at equilibrium.

The scalar σ in 57b, involving the derivatives of the single component adsorbed phase concentrations q_k^0, is non-positive for non-decreasing single component adsorbed phase

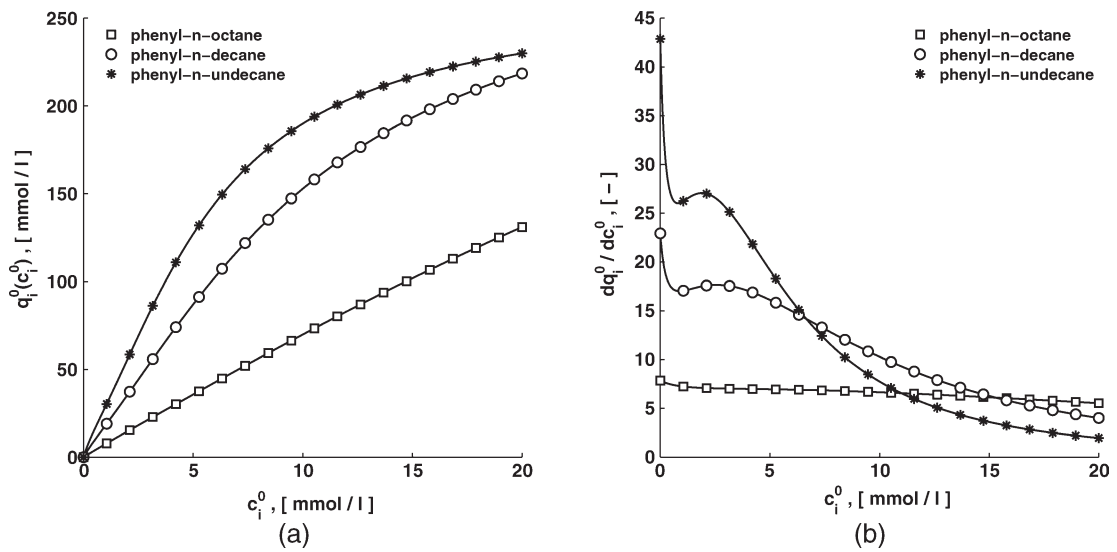

Figure 4. Single component adsorption isotherms of phenyl-*n*-alcanes in the acetonitrile/graphitized carbon system at 50°C taking the parameters of Table 7 as reported by Diack and Guiochon.[22]

(a): Adsorption isotherms. (b): First derivative of the adsorbed phase concentration, q_i^0, with respect to liquid phase concentration, c_i^0.

Table 7. Single Component Adsorption Isotherm Parameters (cf., Eq. 60) of Three Phenyl-*n*-Alcanes for the System Acetonitrile (solvent)/Graphitized Carbon (Porous Adsorbent) at 50°C[21,22]

	q_{i1}^{sat} (mmol/l)	q_{i2}^{sat} (mmol/l)	b_{i1} (l^2/mmol^2)	b_{i2} (l^2/mmol^2)	b_{i3} (l/mmol)
phenyl-*n*-octane	219.4	2.5	0.030	0.0006	0.51
phenyl-*n*-decane	147.2	6.0	0.087	0.010	1.69
phenyl-*n*-undecane	122.4	17.0	0.103	0.032	1.78

concentrations, q_k^0, $k = 1,\ldots,N$. The simple representation (58) is a consequence of the defining Eqs. 9 for the q_i and the fact that these q_i are evaluated along the solution of the equalities given by Eq. 7.

By the representation (58), the inverse of $[\mathcal{I} + \phi\ \mathcal{J}(\boldsymbol{q})]$ can be stated easily with the help of the Sherman-Morrison-Woodbury formula by

$$\left[\mathcal{I} + \phi\ \mathcal{J}(q)\right]^{-1} = \frac{1}{\phi}\mathcal{K}\left(\frac{1}{\phi}\right) \tag{59a}$$

with $\mathcal{K}(\lambda)$ being defined as

$$\mathcal{K}(\lambda) := \mathrm{diag}\left(\frac{c_i^0}{q_{\mathrm{tot}}}\right)\left[\mathcal{I} - K_2(\lambda)\right]\mathrm{diag}\left(\frac{q_{\mathrm{tot}}}{\lambda c_i^0 + q_{\mathrm{tot}}}\right) \tag{59b}$$

for a certain matrix K_2 of rank ≤ 2 (cf., Table 6). Again, all the terms on the right-hand side of (59) are to be evaluated at c. So, $[\mathcal{I} + \phi\ \mathcal{J}(q)]^{-1}$ is given analytically and it is to be evaluated at the given concentrations $c = (c_1,\ldots,c_N)^T$. Thus, the hypothetical liquid phase concentrations, $c^0 = (c_1^0, \ldots, c_N^0)^T$, should be known as functions of c *a priori*. These functions can be calculated efficiently with the alternative new approach explained in the previous section. These analytical formulas can easily be embedded into the numerical approximations that are used to solve the dynamic model equations, resulting in rather accurate computational routines.

It is clear why it is advantageous to have the explicit expressions 58 and 59. The dynamic equilibrium-based models require information of the partial derivatives of the adsorption equilibrium functions. These derivatives are provided analytically by the above expressions 58 and 59. These are applicable regardless of the method used to compute the hypothetical liquid concentrations $c^0 = (c_1^0, \ldots, c_N^0)^T$, that is, the way how the IAST equilibrium problem is solved. The following example illustrates the application of these analytical expressions for $[\mathcal{I} + \phi\mathcal{J}(q)]^{-1}$.

Example 5: adsorber dynamics

We calculate effluent concentration profiles in a liquid chromatography column for mixtures of phenyl-*n*-alcanes in the system acetonitrile/graphitized carbon at 50°C, reported by Diack and Guiochon.[21,22] The adsorption of these solutes is well represented by the combined quadratic plus Langmuir model

$$q_i^0(c_i^0) = q_{i1}^{sat}\frac{c_i^0\left(b_{i1} + 2\ b_{i2}\ c_i^0\right)}{1 + b_{i1}\ c_i^0 + b_{i2}\ c_i^{0^2}} + q_{i2}^{sat}\ \frac{b_{i3}\ c_i^0}{1 + b_{i3}\ c_i^0}, \qquad i = 1, \ldots, N \tag{60}$$

with modified spreading pressure

$$\Pi(c_i^0) = q_{i1}^{sat}\ \ln\left[1 + b_{i1}\ c_i^0 + b_{i2}\ c_i^{0^2}\right] + q_{i2}^{sat}\ \ln\left[1 + b_{i3}\ c_i^0\right] \tag{61}$$

Figure 4 shows the single component adsorption isotherms for phenyl-*n*-octane, phenyl-*n*-decane, and phenyl-*n*-undecane, together with the corresponding slopes, clearly indicating the presence of one or two inflection points in the courses of the adsorption isotherms. The parameters used are given in Table 7. As we do not have an analytical solution to the IAST equations for this case, we resort to the new approach to compute the necessary adsorption equilibria.

Figure 5 presents the orbit $c_2^0(c_1^0)$ for this system and the calculated adsorbed phase concentrations at equilibrium, which reveal the effect of the inflection points of the single component isotherms.

To model the chromatographic column, we discretize the partial differential equations of the equilibrium dispersive model (Eqs. 56, 52b, and 52c) using a *method of lines* approach (i.e., we discretize the spatial domain only, assuming a continuous time domain). We apply a *cell-centered* finite volume discretization with a total number of equally sized cells, n_{cell}, on (56), yielding for a cell j

$$\frac{d\bar{c}(t)_j}{dt} = \left(\left[\mathcal{I} + \phi\ \mathcal{J}\right]^{-1}\right)_j\left[-\frac{1}{\Delta z}\left(\hat{f}_{j+\frac{1}{2}} - \hat{f}_{j-\frac{1}{2}}\right) + D_{\mathrm{app}}\frac{\bar{c}_{j+1} - 2\bar{c}_j + \bar{c}_{j-1}}{\Delta z^2}\right], \quad j = 1, \ldots, n_{\mathrm{cell}} \tag{62a}$$

where $\hat{f}_{j+\frac{1}{2}}$, $\hat{f}_{j-\frac{1}{2}}$ are numerical flux functions at cell j boundaries that depend on the computed flux averages f_j (i.e., $f_j \equiv u\bar{c}_j$). We use the third-order upwind-biased ($\kappa = \frac{1}{3}$)-scheme, applying the limiter recommended by Koren[23,24]

$$\hat{f}_{j+\frac{1}{2}} = f_j + \frac{1}{2}\theta(r_{j+\frac{1}{2}}) \cdot \left[f_j - f_{j-1}\right] \tag{62b}$$

The limiter function, $\theta(r_{j+\frac{1}{2}})$, prevents spurious oscillations under the presence of discontinuities (e.g., shocks) by monitoring the ratio of consecutive cell average gradients, given by $r_{j+\frac{1}{2}} = \frac{f_{j+1} - f_j + \varepsilon_d}{f_j - f_{j-1} + \varepsilon_d}$. ε_d is a small positive constant ($\varepsilon_d \simeq 1 \times 10^{-10}$) to avoid divisions by zero. The computation of the numerical flux functions for a cell j depends only on the cell values of the *compact stencil* $\{j - 1, j, j + 1\}$. The diffusion operator $\frac{\partial^2 c}{\partial z^2}$ is discretized with a standard central difference. We integrate the resulting system of ODEs (62a) with an explicit third-order Runge-Kutta scheme.[23–25]

Simulation results for an equimolar, rectangular pulse injection of phenyl-*n*-octane and phenyl-n-decane are shown in Figure 6. We selected simulation parameters that produce overloading conditions in the column, so that we can observe the competitive effects among solutes at the column outlet. The dynamic concentration profiles show the strong competitive elution behavior of the solutes, as predicted by IAST. The shape of the single component adsorption isotherm model used, that is, the quadratic plus Langmuir model, can be appreciated in the course of the concentration profiles. The

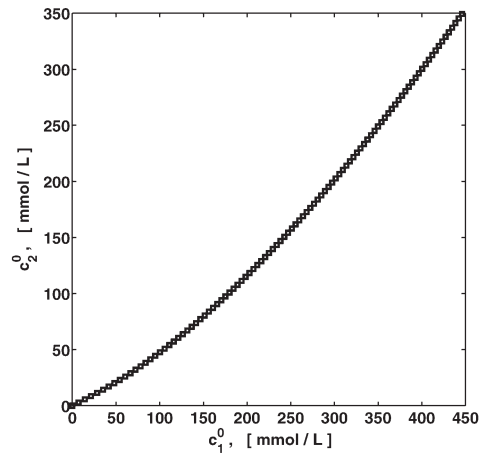

(a) $c_2^0(c_1^0)$

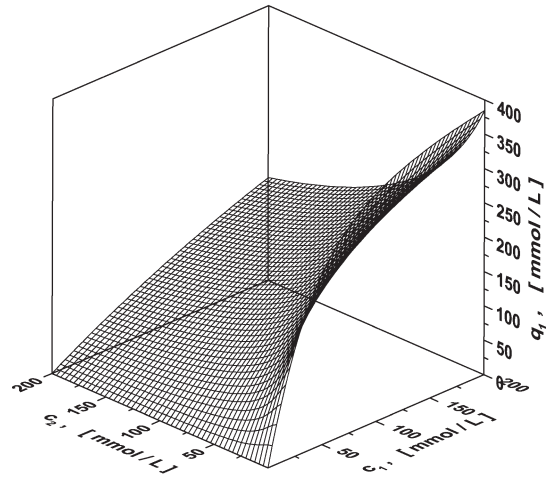

(b) $q_1(c_1, c_2)$

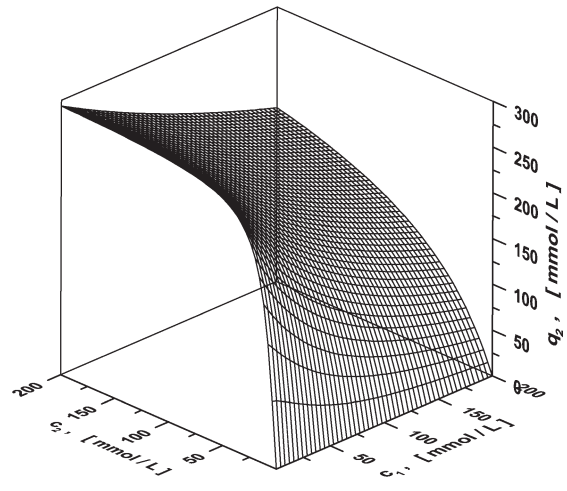

(c) $q_2(c_1, c_2)$

Figure 5. Adsorbed phase equilibrium concentrations for a binary system of phenyl-*n*-alcanes in the acetonitrile/graphitized carbon system at 50°C as predicted by IAST.

(a) Orbit, (b) Component 1: phenyl-*n*-octane, and (c) Component 2: phenyl-*n*-decane. Adsorption isotherm parameters as reported in Table 7.

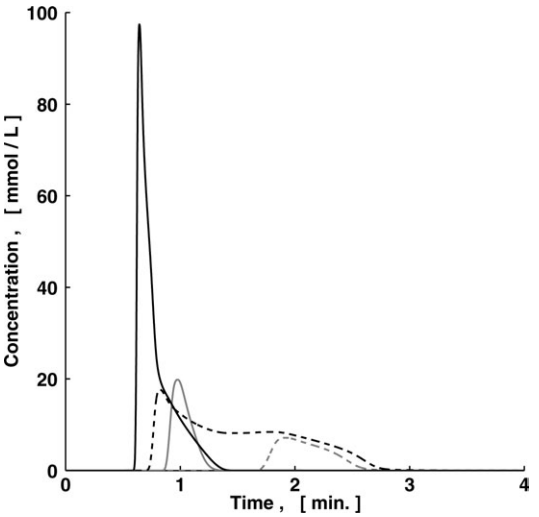

Figure 6. Computed elution profiles corresponding to a rectangular pulse injection of an equimolar mixture of phenyl-*n*-octane and phenyl-*n*-decane for the acetonitrile/graphitized carbon system at 50°C using IAST.

The profiles were calculated with the equilibrium dispersive model and using the analytical expressions for $[\mathcal{I} + \phi\mathcal{J}(\boldsymbol{q})]^{-1}$. Black lines: injection time = 0.2 min. Gray lines: injection time = 0.05 min. Continuous lines: phenyl-*n*-octane. Dotted lines: phenyl-*n*-decane. Simulation parameters: L = 3.0 cm, u = 7.8145 cm/min, ϕ = 0.2987, D_{app} = 0.0117 cm^2/min (same for both compounds), c_{in} = 80.0 mmol/l (for each solute). Adsorption isotherm parameters as given in Table 7.

effect of the inflection points is documented by the unusual shapes of the trailing edges of the peaks. We observe a long trailing edge of the elution peaks at low concentration values, which is typical for compounds obeying a Langmuir-type behavior. This is particularly notable for the most-retained solute. On the other hand, the leading edges of the peaks have an anti-Langmuirian character at intermediate concentration values, thus reducing the sharpness of the front. At higher concentration values, steeper fronts appear. This is particularly notable for the peak of the least-retained phenyl-*n*-octane.

Figure 7 illustrates six predicted effluent concentration profiles for both adsorption ($c_{in} > c_0$) and desorption ($c_{in} < c_0$) processes. Three different concentration levels of equimolar mixtures of phenyl-*n*-octane and phenyl-*n*-decane were considered (2.0, 20.0, and 80.0 mmol/l). The sequence of the calculated adsorption curves (Figures 7a, c, e) reveals the typical displacement of the weaker adsorbed phenyl-*n*-octane and significant front sharpening known for favorable isotherms. A rather large overshoot is predicted for the highest feed concentration (Figure 7e). More interesting are the shapes of the predicted corresponding desorption curves (Figures 7b, d, f). Because of the inflection point in the isotherm course of phenyl-*n*-decane (Figure 4), there is an overshoot of this component in the desorption profile obtained for c_0 = 2.0 mmol/l (Figure 7b). This sometimes already observed phenomenon, is not present anymore for higher concentrations. However, the presence of inflection points in the isotherm of phenyl-*n*-decane can still be recognized in

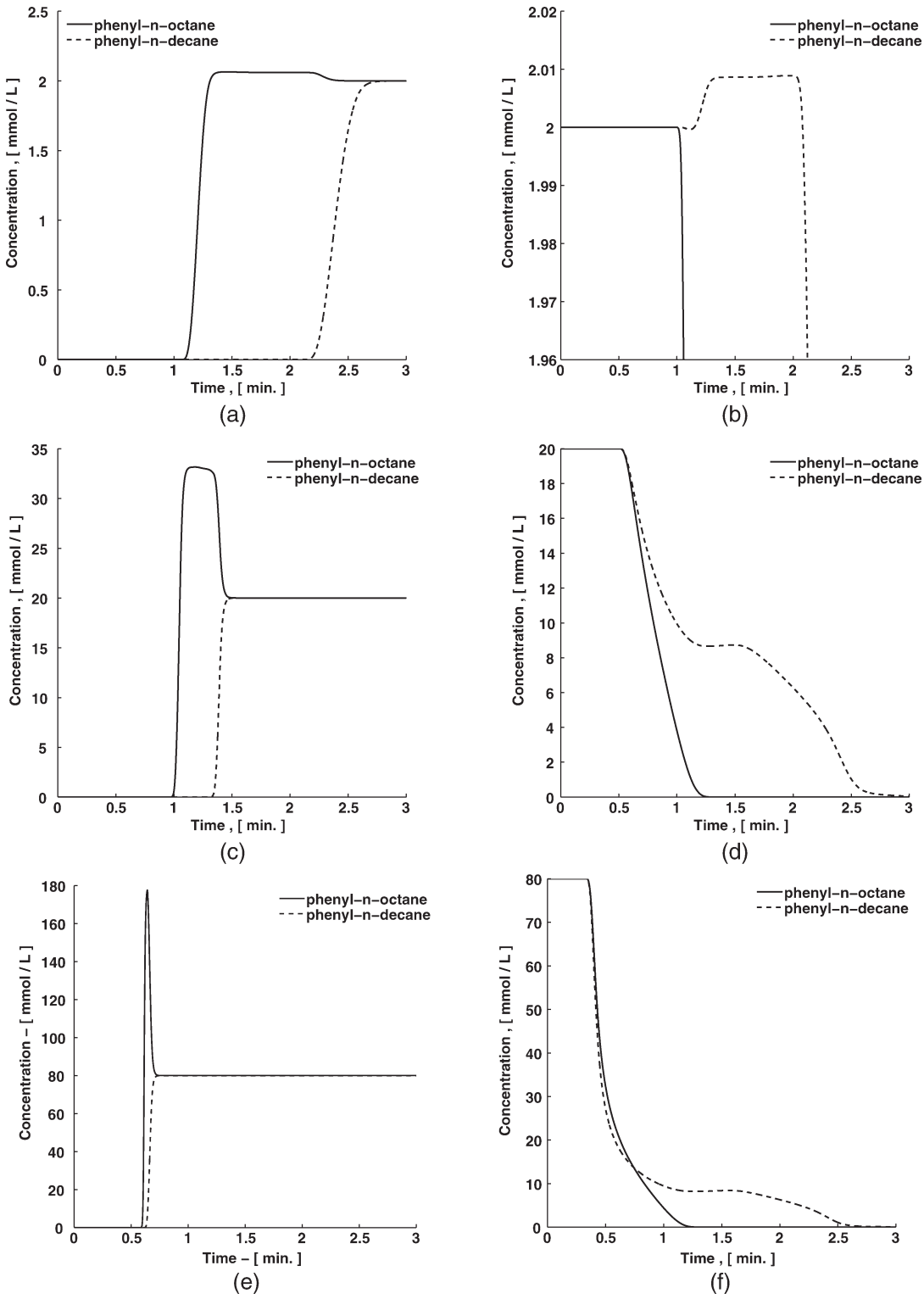

Figure 7. Computed dynamic concentration profiles at the column outlet (i.e., $z = L$) of equimolar amounts of phenyl-*n*-octane and phenyl-*n*-decane for the acetonitrile/graphitized carbon system at 50°C using the equilibrium dispersive model and IAST.

Left column ((a), (c), (e)): adsorption. Right column ((b), (d), (f)): desorption. Inlet (i.e., c_{in}) or initial (i.e., c_0) concentrations: (a), (b): 2.0 mmol/l; (c), (d): 20.0 mmol/l; (e), (f): 80.0 mmol/l. Simulation parameters: $L = 3.0$ cm, $u = 7.8145$ cm/min, $\phi = 0.2987$, $D_{app} = 0.0234$ cm^2/min (same for both compounds). Single component adsorption isotherm parameters as given in Table 7.

the shape of the corresponding elution profile obtained for $c_0 = 20.0$ mmol/l. At the highest concentration level ($c_0 = 80.0$ mmol/l, Figure 7f), the complex equilibrium behavior causes an unusual selectivity reversal.

Further calculations of effluent concentration profiles were performed for binary mixtures of phenyl-*n*-octane and phenyl-*n*-tridecane using various approaches. The results are not shown here for brevity. However, it is important to note that

we experienced convergence problems in attempting to compute these profiles using the standard approaches of O'Brien and Myers and Myers and Do.

Conclusion

In this article, we have introduced a new efficient approach to solve the IAST equations. This approach uses the problem structure and it solves the adsorption equilibrium equations in a dynamic fashion, where a single "decoupled" initial value problem of size N is solved. The solution of this initial value problem provides hypothetical liquid phase equilibrium concentrations $c^0 = (c_1^0, \ldots, c_N^0)^T$ for given $c = (c_1, \ldots, c_N)^T$ and given single adsorption isotherms $q_k^0(c_k^0)$, $k = 1, \ldots, N$. These isotherms can be of arbitrary shape, as long as they satisfy 27. We note that these isotherms might be given by experimental data that are smoothly interpolated as long as the resulting functions are nondecreasing and obeying 27. With this information, we can directly calculate the adsorbed phase concentrations at equilibrium, $q = (q_1, \ldots, q_N)^T$. The calculation of the spreading pressure is avoided, as well as the inversion of $\Pi(c_i^0)$. We would like to emphasize that, in contrast to conventional strategies, our new approach does not need a suitable vector of starting values, $c^{0,\text{start}}$, to compute the sought adsorption equilibria. The advantages of the new approach should be in particular valuable in case where many equilibrium states need to be computed. Furthermore, with respect to calculation of fixed-bed adsorber dynamics within the IAST framework, we provide analytical expressions for the Jacobian of the adsorbed phase concentration functions and for the inverse of $[\mathcal{I} + \phi\mathcal{J}(q)]$. These expressions are applied in the simulation of fixed-bed adsorber dynamics using equilibrium-based models. The hypothetical liquid phase equilibrium values $c^0 = (c_1^0, \ldots, c_N^0)^T$ are the inputs required. We hope this approach will be helpful to further promote IAST.

Literature Cited

1. Ruthven DM. *Principles of Adsorption and Adsorption Processes*. New York: Wiley-Interscience, 1984.
2. Seidel-Morgenstern A. Experimental determination of single solute and competitive adsorption isotherms. *J Chromatogr A*. 2004;1037: 255–272.
3. Myers AL, Prausnitz JM. Thermodynamics of mixed-gas adsorption. *AIChE J*. 1965;11:121–127.
4. Radke CJ, Prausnitz JM. Thermodynamics of multi-solute adsorption from dilute liquid solutions. *AIChE J*. 1972;18:761–768.
5. Suwanayuen S, Danner RP. Vacancy solution theory of adsorption from gas mixtures. *AIChE J*. 1980;26:76–83.
6. Jaroniec M, Madey R. *Physical Adsorption on Heterogeneous Solids*. Amsterdam, New York: Elsevier Science, 1988.
7. O'Brien JA, Myers AL. Rapid calculations of multicomponent adsorption equilibria from pure isotherm data. *Ind Eng Chem Process Des Dev*. 1985;24:1188–1191.
8. O'Brien JA, Myers AL. A comprehensive technique for equilibrium calculations in adsorbed mixtures: the generalized FastIAS method. *Ind Eng Chem Res*. 1988;27:2085–2092.
9. Valenzuela DP, Myers AL. *Adsorption Equilibrium Data Handbook. Prentice Hall Advanced Reference Series*. Englewood Cliffs, NJ: Prentice Hall, Inc. 1989.
10. Myers AL, Valenzuela D. Computer algorithm and graphical method for calculating adsorption equilibria of gas mixtures. *J Chem Eng Jpn*. 1986;19:392–396.
11. Do DD. *Adsorption Analysis: Equilibria and Kinetics. Series on Chemical Engineering* Vol. 2. London: Imperial College Press, 1998.
12. Ilić M, Flockerzi D, Seidel-Morgenstern A. A thermodynamically consistent explicit competitive adsorption isotherm model based on second-order single component behaviour. *J Chromatogr A*. 2010;1217:2132–2137.
13. Tarafder A, Mazzotti M. A method for deriving explicit binary isotherms obeying the ideal adsorbed solution theory. *Chem Eng Technol*. 2012;35:102–108.
14. Kidnay AJ, Myers AL. A simplified method for the prediction of multicomponent adsorption equilibria from single gas isotherms. *AIChE J*. 1966;12:981–986.
15. Moon H, Tien C. Further work on multicomponent adsorption equilibria calculations based on the ideal adsorbed solution theory. *Ind Eng Chem Res*. 1987;26:2042–2047.
16. Redlich O, Peterson DL. A useful adsorption isotherm. *J Phys Chem*. 1959;63:1024.
17. Seidel A, Reschke G, Friedrich S, Gelbin D. Equilibrium adsorption of two-component organic solutes from aqueous solutions on activated carbon. *Adsorption Sci Technol*. 1986;3:189–199.
18. Perry RH, Green DW, editors. *Perry's Chemical Engineers' Handbook*, 8th ed. New York: McGraw-Hill, 2008.
19. Guiochon G, Felinger A, Shirazi DG. *Fundamentals of Preparative and Nonlinear Chromatography*, 2nd ed. Amsterdam, Boston: Academic Press, 2006.
20. Santos JC, Cheng Y, Dias MM, Rodrigues AE. Surface B-splines fitting for speeding up the simulation of adsorption processes with IAS model. *Comput Chem Eng*. 2011;35:1186–1191.
21. Diack M, Guiochon G. Adsorption isotherm and overloaded elution profiles of phenyldodecane on porous carbon in liquid chromatography. *Anal Chem*. 1991;63:2608–2613.
22. Diack M, Guiochon G. Adsorption isotherms and overloaded elution profiles of phenyl-n-alcanes on porous carbon in liquid chromatography. *Langmuir*. 1992;8:1587–1593.
23. Koren B. A robust upwind discretization method for advection, diffusion and source terms. Tech. Rep. NM-R9308, Centrum voor Wiskunde en Informatica - Department of Numerical Mathematics, 1993.
24. Hundsdorfer W, Koren B, van Loon M, Verwer JG. A positive finite-difference advection scheme. *J Comput Phys*. 1995;117:35–46.
25. Shu CW. Total variation diminishing time discretizations. *SIAM J Sci Stat Comput*. 1988;9:1073–1084.
26. Bogacki P, Shampine LF. A (3)2 pair of runge-Kutta formulas. *Appl Math Lett*. 1989;2:321–325.
27. Dormand JR, Prince PJ. A family of embedded Runge-Kutta formulae. *J Comp Appl Math*. 1980;6:19–26.
28. Gear CW. *Numerical initial value problems in ordinary differential equations*. Englewood-Cliffs, NJ: Prentice-Hall, 1971.

Appendix A: Implementation of 32 and 33

For a more compact notation and the practical implementation of the initial value problem 32 and the closure condition 33, we can introduce a running variable ξ with

$$\frac{dc_1^0}{d\xi} = 1, \quad c_1^0(0) = 0 \tag{A1}$$

To bring in the closure condition 33 into 32, we introduce the cut function

$$\text{cut}(c_1^0, \ldots, c_N^0, c_1, \ldots, c_N) = \begin{cases} 1 \text{ for } \left[\prod_{j=1}^{N} c_j^0\right]\left[\sum_{i=1}^{N} \frac{c_i}{c_i^0} - 1\right] > 0 \\ 0, \text{ otherwise} \end{cases} \tag{A2}$$

thus modifying system 32 by a time-scaling to obtain the autonomous initial value problem

$$\frac{dc_1^0}{d\xi} = \text{cut} \tag{A3a}$$

$$\frac{dc_2^0}{d\xi} = \text{cut} \cdot \frac{q_1^0/c_1^0}{q_2^0/c_2^0} \tag{A3b}$$

$$\vdots \tag{A3c}$$

$$\frac{dc_N^0}{d\xi} = \text{cut} \cdot \frac{q_1^0/c_1^0}{q_N^0/c_N^0} \tag{A3d}$$

with initial condition

$$c_k^0(0) = 0, \quad k = 1, \ldots, N \tag{A3e}$$

The prefactor $[\prod_{j=1}^{N} c_j^0]$ in cut is chosen to arrive at a desingularized system A3 avoiding small denominators in $\sum_{i=1}^{N} \frac{c_i}{c_i^0} - 1$. On the region $\{c^0: c_k^0 > 0, \sum \frac{c_k}{c_k^0} > 1\}$ below the surface 33, the orbit of A3 is the same as the solution graph of 32.

Thus, given liquid phase concentrations $c = (c_1, \ldots c_N)^T$, the corresponding adsorbed phase concentrations at equilibrium, $q = (q_1, \ldots, q_N)^T$, can be obtained in the following way:

1. We integrate the initial value problem A3 with the 0 initial value A3e and follow the solution $c^0 = \Psi(\xi)$ of A3 as long as cut is equal to 1. At the instant $\xi = \xi_f(c)$ where cut vanishes, the closure condition 33 is satisfied and the solution becomes stationary: $\Psi(\xi) = \Psi(\xi_f(c))$ for $\xi > \xi_f(c)$. The hypothetical liquid phase concentrations at equilibrium are thus given by $c^0(c) = \Psi(\xi_f(c))$.

2. With these $c^0(c)$ values, we directly define the adsorbed phase equilibrium concentrations, $q(c)$ using Eq. 10.

In summary, the cut-function is monitoring the closure condition: As long as the solution of A3 is "below", the closure surface, one moves "upwards", until the cut-function vanishes for the first time.

When passing from a set of liquid concentrations $c = (c_1, \ldots c_N)^T$ to another one $\hat{c} = (\hat{c_1}, \ldots \hat{c_N})^T$, we might replace the initial value 0 in A3e by $c^0(c)$. In case of $\sum \frac{\hat{c}_k}{c_k^0(c)} > 1$, the system A3a–A3d remains unchanged whereas in case of $\sum \frac{\hat{c}_k}{c_k^0(c)} < 1$, the definition of cut in (A3a)–(A3d) is to be changed to

$$\text{cut}(c_1^0, \ldots, c_N^0, c_1, \ldots, c_N) = -1 \quad \text{for} \left[\prod_{j=1}^{N} c_j^0\right]\left[\sum_{i=1}^{N} \frac{c_i}{c_i^0} - 1\right] < 0$$

and $\text{cut}(c_1^0, \ldots, c_N^0, c_1, \ldots, c_N) = 0$ otherwise, to account for the reversed direction of integration.

Under our assumptions on the single component isotherms $q_i^0(c_i^0)$, in particular under $q_i^0(0) = 0$ and $\frac{dq_i^0}{dc_i^0}(0) > 0$, the right-hand side of A3a–A3d is well-defined at the origin $c^0 = 0$ so one can prescribe the initial value (A3e). In case a single component isotherm $q_i^0(c_i^0)$ has $c_i^0 = 0$ as a zero of order > 1 and in case of an isotherm having infinite slope at $c_i^0 = 0$, the initial value A3e cannot be used. Here, preliminary blow-up transformations lead to a desingularization of the initial value problem A3.

Appendix B: Properties of the Jacobian

We now prove the hyperbolicity of the Jacobian $\mathcal{J}(q)$, mentioned in section entitled Dynamic Modeling of Fixed-Bed Adsorbers Using IAST, in two steps.

Proposition A. *The Jacobian $\mathcal{J}(q)$, given in Eqs.* 58a, *and* 58b, *is a hyperbolic matrix with N positive eigenvalues and N linearly independent eigenvectors in case of strictly increasing single component isotherms q_k^0, $k = 1,\ldots,N$.*

Proof.

- Step 1 (Real eigenvalues/Symmetrization): One has

$$\lambda I + \mathcal{J}(q) = D^{-1}(\lambda)\big(I + H(\lambda)\big)\Delta = D^{-1}(\lambda)\Delta + H(0)\Delta \tag{B1a}$$

with the diagonal matrices $D = D(\lambda)$ from Table 6 and $\Delta = \text{diag}\ (\delta_k)$, $\delta_k := q_{\text{tot}}/c_k^0$. We recall $D(0) = I$ and $d \equiv \text{col}\ (d_k)$ with $d_k \in (0,1]$. The matrix $H = H(\lambda)$ is also given in Table 6, and $H(0)$ allows the following factorization:

$$\begin{aligned} H(0)\Delta &= X\big((e^T W^2 x - \sigma)e^T - w^T\big)\Delta - Wxe^T\Delta \\ &= X\big((e^T W^2 x - \sigma)ee^T - ew^T - we^T\big)\Delta \\ &= \big(X\Delta^{-1}\big)^{1/2}\big[\big(\Delta X\big)^{1/2}\big((e^T W^2 x - \sigma)ee^T - ew^T - we^T\big) \\ &\quad \times \big(\Delta X\big)^{1/2}\big]\big(X\Delta^{-1}\big)^{-1/2} \end{aligned} \tag{B1b}$$

since the various diagonal matrices can be freely intertwined. Hence $\lambda I + \mathcal{J}(q)$ is similar to a symmetric matrix, so it has N real eigenvalues with N linearly independent eigenvectors.

- Step 2 (Positive eigenvalues): We now show that $\lambda I + \mathcal{J}(q)$ is invertible for all real $\lambda \geq 0$ which implies that $\mathcal{J}(q)$ has only positive eigenvalues. Because of B1a, this will follow from a nonzero $(I + H(\lambda))$. With the definitions from Table 6, suppressing the λ-dependences, and with

$$f^T D = (w^T W x - \sigma)d^T - w^T D = (e^T W^2 x - \sigma)d^T - d^T W$$

one arrives at

$$\begin{aligned} &\det\big(I + H\big) = \det\begin{bmatrix} 1 - e^T DWx & -e^T Dx \\ f^T DWx & 1 + f^T Dx \end{bmatrix} \\ &= 1 - e^T DWx + f^T Dx - e^T DWx \cdot f^T Dx + e^T Dx \cdot f^T DWx \\ &= 1 - d^T Wx + d^T\big(\big[(e^T W^2 x - \sigma)I - W\big)\big]\big[x + (d^T x)Wx - (d^T Wx)x\big] \\ &= 1 - d^T Wx + d^T\big((e^T W^2 x)I - W\big)\big[x + (d^T x)Wx - (d^T Wx)x\big] - \sigma d^T x \\ &= 1 - 2d^T Wx + e^T W^2 x \cdot d^T x - d^T x \cdot d^T W^2 x + (d^T Wx)^2 - \sigma d^T x \\ &= \big(1 - d^T Wx\big)^2 + d^T x\big(e^T - d^T\big)W^2 x - \sigma d^T x \end{aligned} \tag{B2}$$

Therefore, this determinant is positive for all $d_k \in (0,1]$ in case of a negative σ, given by

$$\sigma = \sum_{k=1}^{N} w_k\ c_k\ q_{\text{tot}} \frac{d}{dc_k^0}\frac{1}{q_k^0} \tag{B3}$$

according to Table 6. The first two summands in the last line of B2 are always positive with the only exception $D = I$, that is, $\lambda = 0$, where one has $(I + H(0)) = -\sigma$. It is obvious by B3 that strictly increasing q_k^0 entail a negative σ.

Remark. *A weaker sufficient condition for σ in* (B3) *to be negative is the following one*:

(☆) *Each single component adsorbed phase concentration function q_k^0 is nondecreasing and there does not exist a point c where all q_k^0, considered as functions of c along the IAST-solution, vanish simultaneously.*

Of course, this statement is just a trivial sufficient condition for a positive det $(I + H)$ and by no means a necessary

Table 8. Maximum Absolute Errors, e_c^{abs} and Relative Errors, e_c^{rel}, Obtained for $\hat{q}_1$ using ode45 for Different Tolerance Values

Relative Tolerance (RelTol)	Absolute Tolerance (AbsTol)	e_c^{abs} (g/l)	e_c^{rel} (−)
10^{-3} (default)	10^{-6} (default)	1.2×10^{-4}	2.0×10^{-4}
10^{-5}	10^{-8}	3.3×10^{-6}	3.9×10^{-6}
10^{-10}	10^{-12}	9.5×10^{-9}	9.8×10^{-10}
10^{-13}	10^{-14}	9.5×10^{-9}	9.8×10^{-10}

one. Analyzing the proof of Proposition A, the condition ($\bigstar$) *turns out to be sufficient for* $\mathcal{J}(q)$ *to be hyperbolic with N positive eigenvalues.*

Appendix C: ODE Solvers

It is important to underline that the performance of the new approach directly depends on the type of numerical integration method used to solve the resulting initial value problem. In order to illustrate this, three different ODE solvers available in MATLAB were chosen:

- ode23 (one-step, Bogacki-Shampine 3(2) Runge-Kutta pair[26]),
- ode45 (one-step, Dormand-Prince 5(4) Runge-Kutta pair[27]) and
- ode15s (multistep, variable order Backward Differentiation Formulae[28])

Additionally, each solver allows for different values of absolute (AbsTol) and relative (RelTol) error tolerances. As the resulting initial value problem assembled with the quadratic single component adsorption isotherm discussed in Example 2 is not stiff, we observed that all three solvers performed well under default tolerances, with similar values for the calculated errors, as compared to the reference (i.e., analytical) solution. Setting stringent relative and absolute error tolerances on these solvers directly affects the attainable local error of the integrated solution (for prescribed orders of accuracy of the chosen integrators), as well as the number of function evaluations (i.e., computational cost) required to meet these error tolerances. Table 8 illustrates the effect of the error tolerances on the accuracy of the solution using the ode45 solver. For brevity, we do not present the errors of ode23 and ode15s, which displayed a similar behavior.

Manuscript received Dec. 5, 2011, and revision received July 18, 2012.